5-1-2015

# PETTINGER ENGINE ANALYSIS AND IMPROVEMENT

Amir Shrestha

# PETTINGER ENGINE ANALYSIS AND IMPROVEMENT

by

AMIR SHRESTHA

Presented to the Faculty of the Honors College of

The University of Texas at Arlington in Partial Fulfillment

of the Requirements

for the Degree of

HONORS BACHELOR OF SCIENCE IN MECHANICAL ENGINEERING

THE UNIVERSITY OF TEXAS AT ARLINGTON

May 2015

ACKNOWLEDGMENTS

First, I would like to thank Mr. Wesley Pettinger, who is the sponsor of this design project, for providing us the wonderful opportunity of working on such an exciting project. Next, I would like to thank Dr. Raul Fernandez and Dr. Robert L. Woods, the faculty mentors of this project, for providing valuable suggestions and support for completing this project. Next, I would like to express my acknowledgements to my team members Michael Araujo, Robin Pittsley, Brandon Allen, and Mauro Guadiana without whom this project could not have been completed. Finally, I would like to thank the Mechanical and Aerospace Engineering Department and The Honors College for providing whatever support was possible.

May 25, 2015

# ABSTRACT

## PETTINGER ENGINE ANALYSIS AND IMPROVEMENT

Amir Shrestha, ME

The University of Texas at Arlington, 2015

Faculty Mentors: Raul Fernandez and Robert L. Woods

The Pettinger Engine is a six link internal combustion engine that has a very different kinematics than a conventional engine. Its prototype was developed by Mr. Pettinger; however, its true capabilities are yet to be discovered. We were given the task of quantifying the capabilities of this engine. Various analyses were done to find engine characteristics and performance while comparing the results to a conventional engine. Variable valve timing and throttle elimination were also implemented to increase engine performance. Torque and angularity calculations showed more promising results in favor of the Pettinger Engine. Friction calculations revealed to have not much effect on the torque. Variable valve timing allowed for a greater expansion ratio and throttle elimination allowed for removal of pumping loss and thus more efficiency. Overall, the Pettinger Engine has competitive performance when compared to a conventional engine while having a smaller or compact size.

TABLE OF CONTENTS

LIST OF ILLUSTRATIONS

# CHAPTER 1

# INTRODUCTION

## 1.1 The Pettinger Engine

Internal combustion engines have been around for a long time. They have great importance in our lives as they power our vehicles, generators, boats, etc. However, the fundamental design of the engine has not changed much from when it was first developed. Various efforts have been done to make the engine efficient without changing the main design (Pace, Wiggins, Sandberg). Mr. Pettinger, however, wants to increase the productivity of the engine by slightly changing the core design of the engine itself.

The Pettinger Engine is an internal combustion engine that was developed by Mr. Wesley Pettinger, who is our project sponsor. It basically has two extra links than that of a conventional crank-slider engine as can be seen below in figure 1.1.

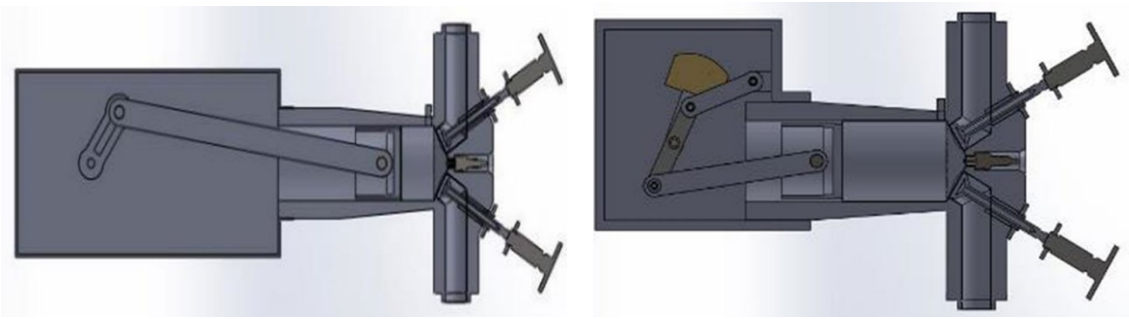

Figure 1.1: Geometric comparison between conventional engine (left) and Pettinger Engine (right)

This special linkage configuration allows for a longer stroke while having a smaller space. Furthermore, since the piston rod of the Pettinger Engine doesn't make much angle with respect to the piston center during the entire cycle, it is expected to have lower

frictional forces as well (Pettinger).

## 1.2 Project Requirements

The Pettinger Engine as developed by Mr. Pettinger is only a prototype engine as of now. When this engine was developed, it was developed more from a trial and error method than a typical engineering design approach. Previous work on doing a complete engineering analysis of this engine includes one that was done by a senior design group before us (SPARC). In our project we try to build on whatever work was done by them.

The first requirement of the project was to compare the capabilities and selected parameters of the Pettinger Engine with that of a conventional engine. It was noted that due to its particular geometry, this engine would be suitable for a variable longer expansion ratio such that Variable exhaust valve timing analysis was also required. Furthermore, to further improve the capabilities of the Pettinger Engine, pumping loss was required to be eliminated by doing intake valve timing analysis.

## 1.3 Project Flowchart and Technical Approach

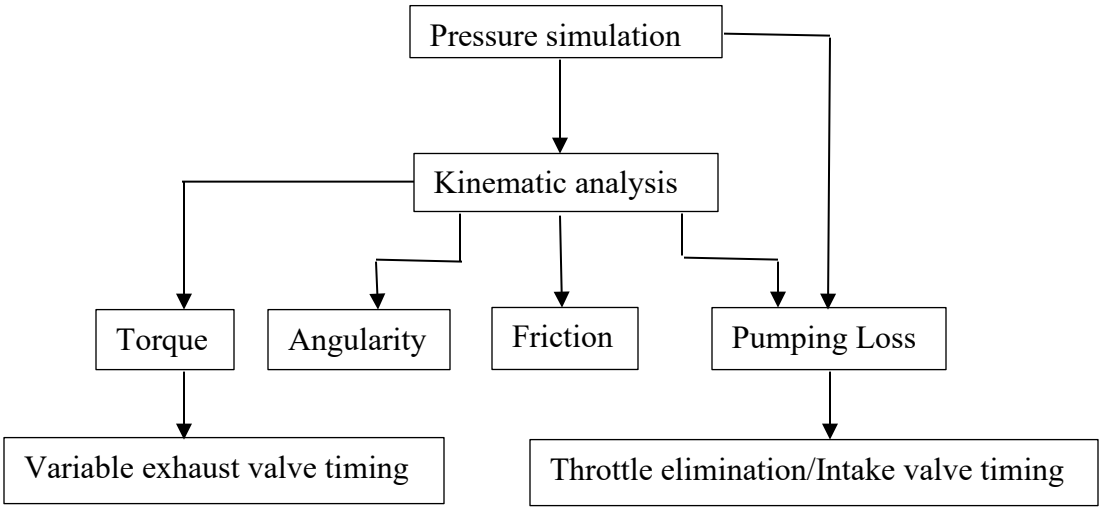


Figure 1.2: Project flowchart

Figure 1.2 is the project flowchart that shows the sequential flow of tasks that were performed in this analytical project. First, the pressure data was required. Although Lotus simulation software was initially chosen to get the pressure data, a completely theoretical model was later used to get the data. Then, kinematic analysis was performed; in particular position analysis was done for both the Pettinger Engine and conventional engine. The position analysis when combined with the pressure data during the force analysis provided various parameters of interest such as torque, piston rod angle, and friction. Piston rod angle and friction were useful for comparison purposes. However, torque was required for not only comparison purposes but also for Variable exhaust valve timing analysis which will be discussed in detail later on. Pumping loss calculation was done to show how much energy is being wasted due to a conventional throttle. It was calculated by obtaining the pressure volume plot through the combination of pressure and kinematic analysis. Finally, throttle elimination analysis was made possible by the implementation of intake valve timing.

CHAPTER 2

# PRESSURE SIMULATIONS

## 2.1 Lotus Simulations

During the first semester of this project a lot of time was invested in getting the pressure data from Lotus simulation software. Many problems were encountered for the results obtained through Lotus, and because of this a completely numerical approach was later used (IES). Some of the problems encountered with Lotus simulations will now be discussed briefly.

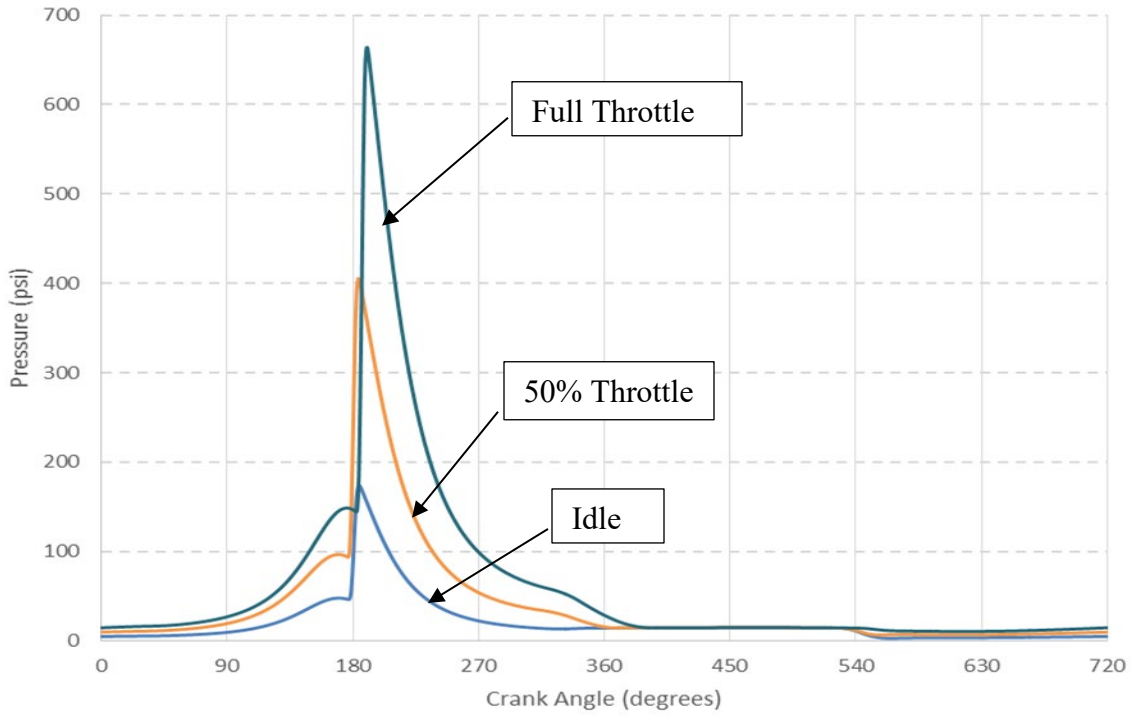


Figure 2.1: Pressure vs crank angle obtained from Lotus simulation with pressure drop problem

Figure 2.1 is one of the several simulations that were performed using Lotus in order to get realistic pressure data for further analysis. The problem encountered during this simulation was a strange pressure drop before the combustion as evident at about 180 degrees in the figure. In reality there should be a smooth transition from compression to combustion curve, and thus this result was considered unacceptable.

Figure 2.2 below is another simulation performed on Lotus. In this figure the Top Dead Center is 360 degrees. In figure 2.1, the problem encountered was an unusual pressure drop before combustion. It was thought that the pressure drop was occurring because ignition timing data was not being put in the simulation model. Ignition timing data was later found from literature for 2000 RPM speed (HR Tuning). However, it was later realized that specific ignition timing data could not be input in Lotus because it did not have that functionality. There was, however, something called a phase angle input which could approximate ignition timing if planned properly (Lotus Cars Ltd.). The ignition timing data was thus input as phase angle and the plot shown in figure 2.2 was generated. It can be seen that the pressure drop before combustion was dramatically reduced. However, a new problem was observed: peak pressure shifting to before TDC. As clearly evident for lower throttle percentages, the peak pressure shifts to before TDC. This is something that is not physical. In reality, it would mean that the maximum pressure is occurring before combustion and in the compression stroke. This is theoretically not possible, and thus this result obtained was also regarded as useless for our purposes.

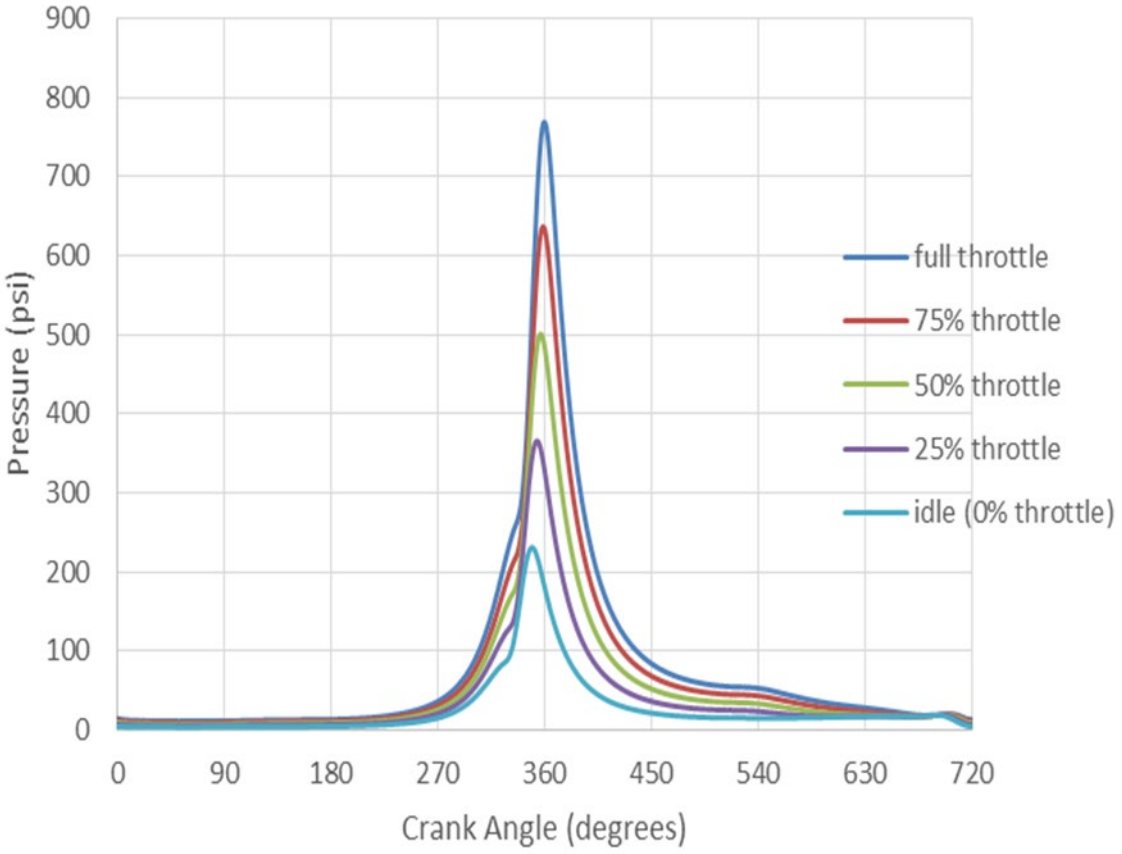


Figure 2.2: Pressure vs crank angle obtained from Lotus simulation showing peak pressure shift problem

Several trial and error and experimentation were done with Lotus to get realistic pressure data, but unfortunately Lotus was not able to give us that data. A completely analytical method was thus utilized later on and Lotus was completely discarded.

## 2.2 The Computational Model of Cylinder Pressure

Paulina Kuo in her research paper provides a very simple method to obtain cylinder pressure using a completely analytical approach that can be easily programmed in programming languages such as MATLAB. The four stroke cycle as found in most internal combustion engines are intake, compression, combustion, expansion, and exhaust. The method of modelling these cycles will now be discussed (Kuo).

Intake stroke:

During this phase, the piston starts at the TDC and moves till the BDC drawing in the air fuel mixture. As told by Kuo in her paper, there is little resistance to gas flow into the cylinder, which causes the pressure in the cylinder to remain relatively constant and equal to the inlet pressure.

Compression:

The compression stroke ideally starts at the BDC. However, in order to achieve a constant compression ratio of 10:1, some of the air is blown out until certain degrees crank angle. The derivation of that specific crank angle where the intake valve is closed can be found in the appendix. Other than this, modelling the compression stroke is simply described by a polytropic equation:

$$PV^n = constant$$

The value of *n* is approximately equal to 1.3.

Combustion:

The combustion process can be described by the mass burn fraction and the Weibe function. According to the McCuiston, Lavoie and Kauffman (MLK) model, the mass burn fraction is given by

$$Xb = \frac{PV^n - PoVo^n}{PfVf^n - PoVo^n}$$

Where,

P = pressure corresponding to burn fraction

V = volume corresponding to burn fraction

Po = pressure at the start of combustion

Vo = volume at the start of combustion

Pf = pressure at the end of combustion

Vf = volume at the end of combustion

n = polytropic constant

The value of n is approximately equal to 1.25 for combustion.

The Weibe function is given by

$$Xb = 1 - \exp\left[-a\left(\frac{\theta - \theta o}{\Delta\theta}\right)^{m-1}\right.$$

Here, θo is the crank angle at the start of combustion, Δθ is the total combustion duration. The end of combustion is usually about 15° aTDC (Pulkrabek), from which Δθ can be found knowing the ignition angle. The value of a = 5 and m = 2 as suggested in Paulino's paper.

The Xb from Weibe function when substituted in the MLK model equation for mass burn fraction and rearranged gives the pressure during combustion as a function of crank angle (θ). There are, however, two unknowns left in the resulting equation to solve for pressure; they are Vf and Pf. Vf can be found once the piston position is known for a specific crank angle. The piston position and the crank angle are related by the geometry of the crank mechanism, which is known. Once piston position for any crank angle is found, Vf can be found by using the formula for volume of a cylinder. Pf can be found from equation of state at the final position of combustion. Still Tf (final temperature of combustion) is needed to solve the equation of state. This can be done by the following equation:

$$m_{total} Cv(Tf - Tspark) = Cm_{fuel} Q_{HV}$$

Where,

$M_{total}$ = total mass of gases in the cylinder

Cv = specific heat of gas mixture at constant volume

Tspark = temperature at the start of combustion

C = coefficient for unburned fuel

$m_{fuel}$ = mass of fuel in the cylinder

$Q_{Hv}$ = heating value of the fuel

The total mass can be found using ideal gas equation of state during start of compression. The value of Cv is equal to that of air and is equal to 1.004 KJ/kg. K at 3000 K, corresponding to the approximate temperature at the end of combustion. The spark temperature can be found using equation of state at the end of compression. The value of C is approximately equal to 0.95. The mass of fuel in the cylinder can be known using the air-fuel ratio and the total mass in the cylinder. The heating value of fuel is about 44 MJ/kg.

Expansion:

The expansion process can also be described simply by a polytropic process as was done for the compression. The value of the polytropic constant is about 1.48 for expansion.

Exhaust:

The exhaust stroke can be described by a flow rate equation. This is a differential equation and is a little complicated to program in MATAB. It also requires the use of three step Runge-Kutta algorithm. Since, for the purposes of this project, we are really interested only untill the expansion phase; the exhaust process was not modelled.

## 2.3 MATLAB Simulation

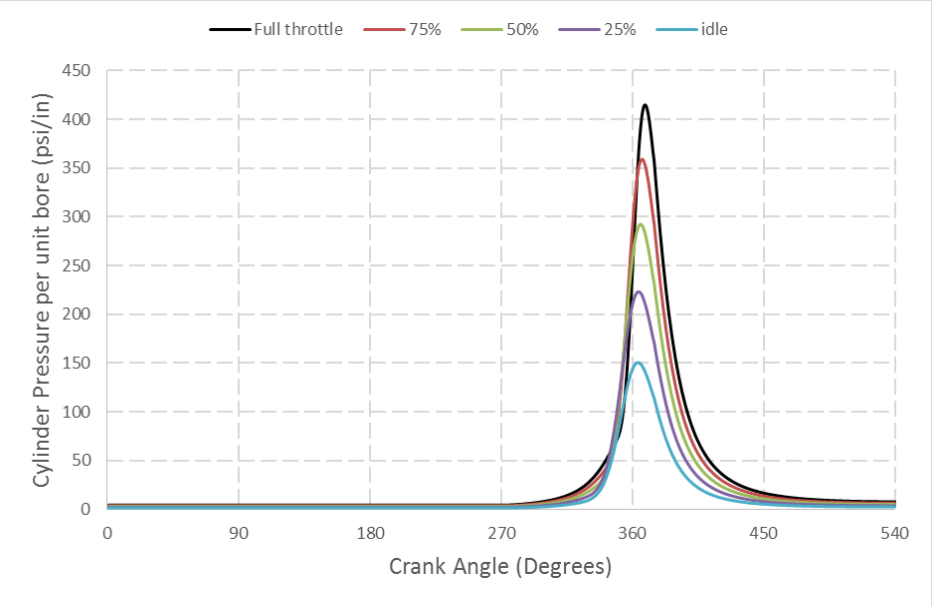


Figure 2.3: Pressure for various throttles levels at a compression ratio of 10:1 at 2000 rpm as obtained from theory and MATLAB

Figure 2.3 is the pressure data obtained through the use of thermodynamic theories and equations described previously. The thermodynamic theories described were implemented in MATLAB and the pressure plot was thus obtained. Although certain assumptions were used during the modeling, this graph is much better than previous graphs obtained through Lotus. The transition from compression to ignition is very smooth. The ignition timing for different throttles are different as was desired, and the peak pressure occurs few degrees after TDC, which was also our requirement. Notice that for lower throttles, the peak pressure starts to shift a little to the left. This is expected phenomena because for lower throttles we are increasing the ignition angle, which means that combustion is taking place early. However, since the peak pressure doesn't occur on or before TDC, the results obtained are acceptable. Since satisfactory results were

obtained through this method of modelling, the later analysis of this project used the data thus obtained.

# CHAPTER 3

# KINEMATIC ANALYSIS

## 3.1 Position and Force Analysis

The kinematic equations that were used to analyze the motion of the Pettinger Engine were composed by forming two six section vector loops of the linkage system. Each link is represented as a vector with its angle measured from the positive X - axis. The vectors that make up the loop are summed up and are set equal to zero. If a vector that makes up part of the loop is drawn in the opposite direction of the flow of the loop, it will be considered negative and thus subtracted from the sum (Norton).

Each vector in the loop is defined by the magnitude of the vector multiplied by the complex polar notation of the angle ($r * e^{j\theta}$). An advantage to using the complex notation to represent planar vectors comes from using the Euler Identity. The Euler Identity can then be separated into its Real and Imaginary components. Another advantage to using complex notation of a planar two-dimensional vector is that it can be easily differentiated or integrated since it is its own derivative and can be used to develop velocity and acceleration data for each link (Norton). The methodology used is shown in the Appendix.

Thus, using this methodology every unknown variable can be known. The solution obtained from the kinematic analysis when combined with the pressure data during the force analysis would eventually give the torque output and other useful data.

Force analysis can be performed simply by applying Newton's second law on each of the linkages. All the rotating components will have three scalar equations i.e. force in the x direction, force in the y direction, and a moment equation. The piston, however, will not have a moment equation because it is only translating. Using some friction constraint, there will be in total 14 simultaneous equations (Norton). It is assumed that the inertia/masses of the linkages are insignificant since the forces produced in the joints are very large such that all the simultaneous equations will have a zero in the right hand side. The simultaneous equations can then be put in the form of a matrix and all the unknowns can be solved quite easily by a simple matrix inversion. The unknowns include the forces in the system and a reaction torque. The details of the force analysis can be found in the Appendix.

## 3.2 Torque Output

During the first semester of the project, torque was calculated for both the conventional engine and the Pettinger Engine. However, much unexpected results were obtained. First, the torque output of both the engines were found to be almost same. Second, the magnitude of the torque values were unrealistically high (IES).

Some doubts remained over the validity of such outrageous results such that the force analysis and MATLAB programming was revisited this semester. It was found that such high magnitude of torque was being obtained because of using unrealistically higher dimensional values, for instance the bore size was used as 5.16 inch and the stroke to bore size was 1.7. These dimensions were obtained from the previous group that worked on this project. The problem with results obtained from these values was that a realistic solution check could not be performed. For example, if the values obtained were close

enough to generally accepted values in the real world, then it could be known if the solution we obtained was correct. For this reason, the bore size was reduced to reasonable 3.26 inch and stroke to bore ratio reduced to a reasonable 1.2. These values were chosen corresponding to the engine model that was described in the computational pressure simulation paper by Kuo. By modifying the bore and the stroke to bore ratio a more realistic torque value was thus obtained.

Furthermore, during the detailed check of the MATLAB code, it was found that a slight typo was made in the code. Fixing this error gave a completely different torque result for the Pettinger Engine than what was obtained last semester.

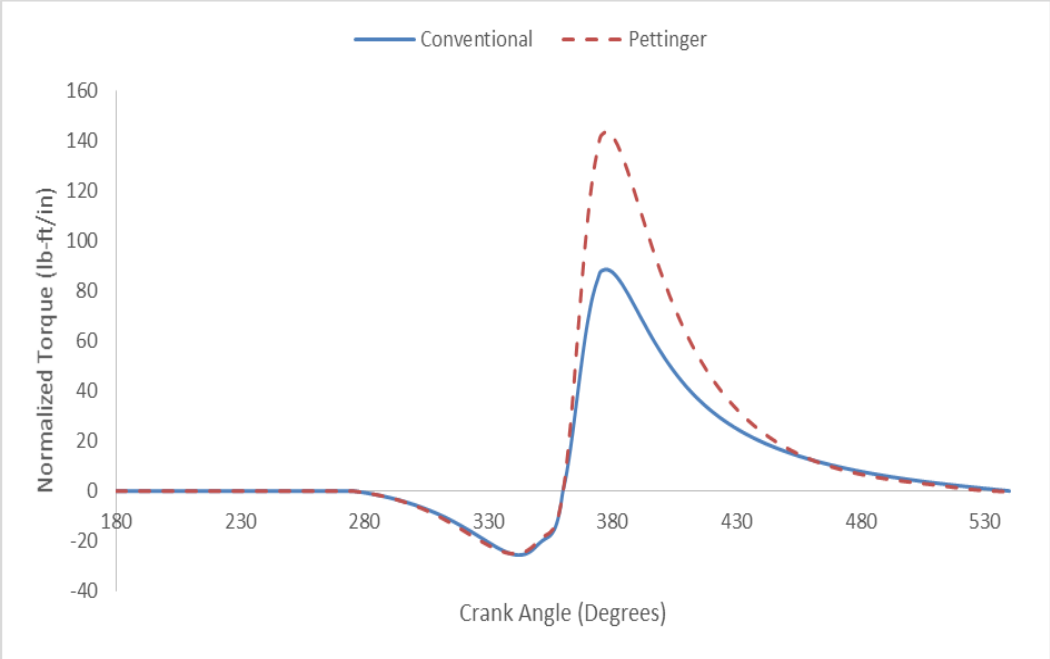


Figure 3.1: Torque vs crank angle comparison for the conventional engine and Pettinger Engine

Figure 3.1 is the result obtained after making the error corrections. It can be clearly seen in the plot that the Pettinger Engine has a higher peak torque than the conventional engine. In fact the peak torque was calculated to be about 62% higher. This

is a promising result because it means that a same size Pettinger Engine would produce more power. This seems to be an obvious advantage. Further analysis of the project included other benefits of the Pettinger Engine and trying to find an analytical justification of the higher torque.

### *3.2.1 Variable Exhaust Valve Timing*

Since the Pettinger Engine can accommodate a longer stroke in a small space, having an expansion ratio larger than the compression ratio would be obviously beneficial. After the torque values were obtained for all the part throttles from full throttle to idle condition, they were plotted in the same graph. Along with the torque values, a constant number was also plotted. This particular number was chosen to be 2% of the maximum torque. The point where this constant line intersected the torque curves for the respective throttles was the cutoff point. The crank angle values corresponding to the cutoff point are the angles where the exhaust valve will be opened. This simple analysis thus provided parameters required to implement Variable exhaust valve timing in the Pettinger Engine.

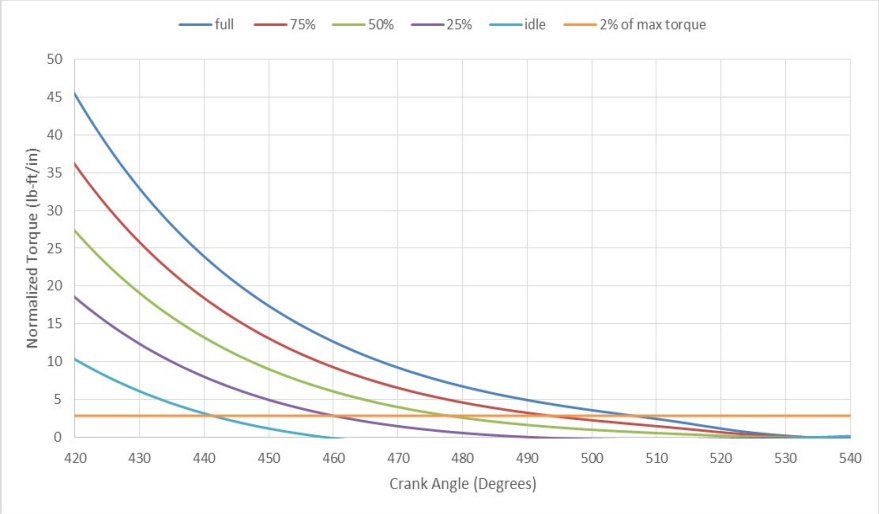


Figure 3.2: Variable valve timing calculation

Figure 3.2 is the torque graph that was used for finding the exhaust valve timing using the methodology as mentioned before. It is important to note that the crank angle of 444 degrees would have been where the exhaust valve would be opened if the expansion ratio and compression ratio were same which is 10:1 for our case. Any more work obtained after that angle is an advantage of using variable expansion ratio, which is more suited to the Pettinger Engine.

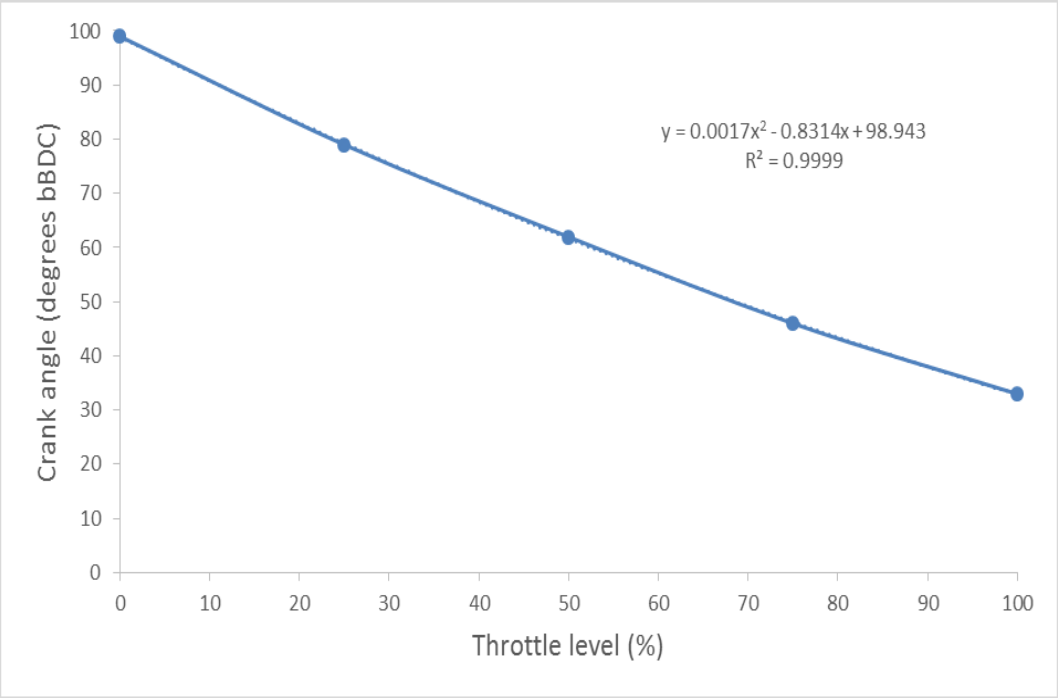


Figure 3.3: Exhaust valve timing vs throttle (%) demand

With the data from figure 3.2, figure 3.3 was plotted. Using this plot as well as the polynomial curve fit equation, exhaust valve timing for any throttle % can be obtained.

## 3.3 Angularity and Friction

The Angularity of the engine is the angle between the piston rod and the centerline of the piston. Looking at the kinematics of the Pettinger Engine, it seemed obvious as though the piston rod angle would be much less than that of the conventional

engine. The angularity values were found very easily from the kinematics equations that was used for the position analysis.

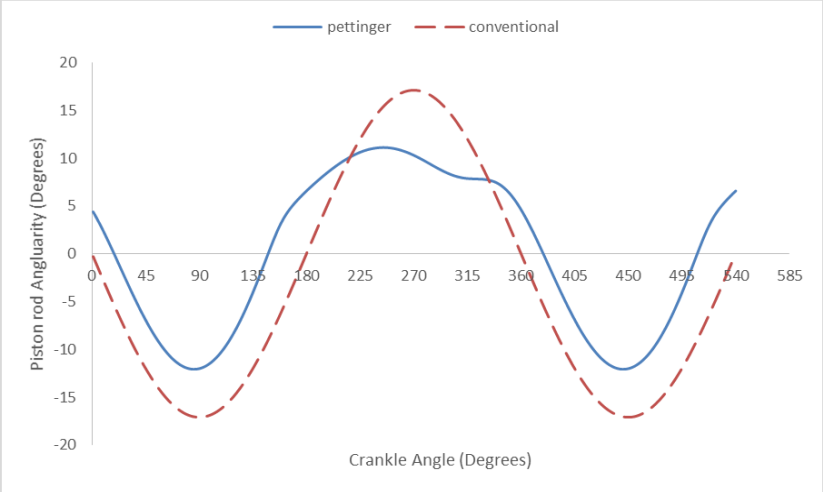


Figure 3.4: Piston rod angularity vs crank angle

From figure 3.4 it can be seen that the piston rod angle of both the engines are quite different from each other. The conventional engine has higher peak angularity than does the Pettinger Engine. Furthermore, the conventional engine has higher angularity than that of the Pettinger Engine for most of the time. The Pettinger Engine has higher angularity values only a few times. The maximum angularity of the conventional engine was found to be about 17 degrees whereas that of the Pettinger Engine was found to be about 12 degrees.

These quite varying angularity plots had much effect on the cylinder wall friction. It is so because the angularity determines how much normal force is transmitted to the piston from the rod which in turn would determine the friction. The friction of the cylinder wall can be found easily from the force analysis that was performed before. From the force analysis, the normal force can be found which when simply multiplied to the coefficient of friction gives the cylinder wall friction.

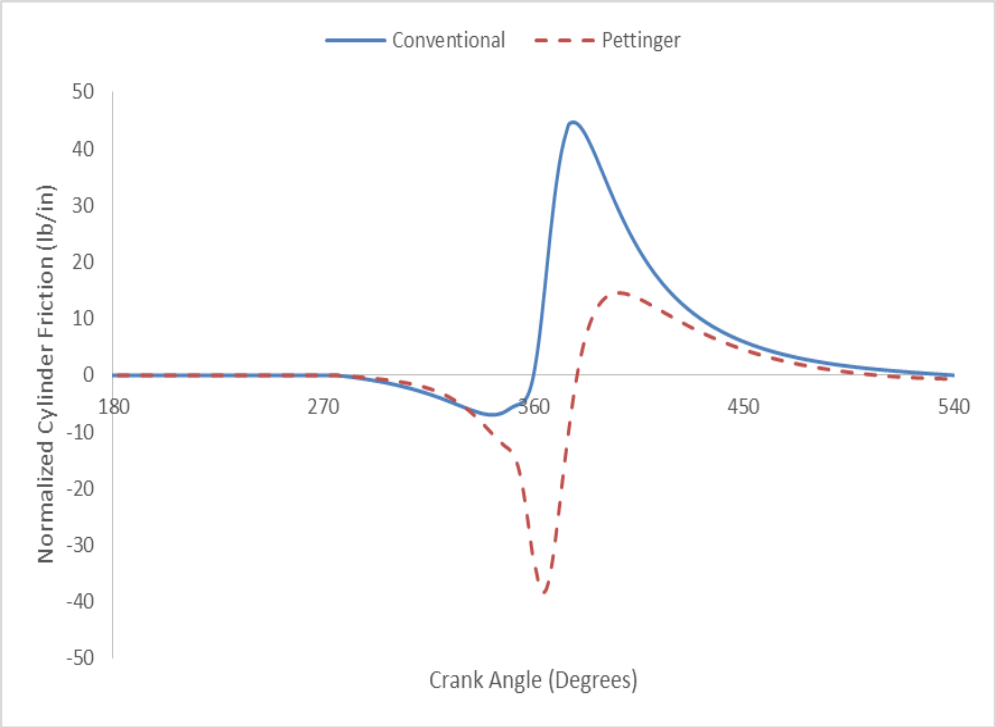


Figure 3.5: Cylinder friction vs crank angle

Figure 3.5 shows the cylinder friction as a function of crank angle. As evident, the friction plot of the both the engines are quite different from each other. This was expected because the angularity plots as seen from figure 3.4 are quite different for both engines. The negative friction seen in the plot signifies that the piston is travelling in the different direction than that of the assigned positive direction. One interesting thing to note is that the conventional engine has a higher friction during the timing of the peak torque. It was again expected because referring to the angularity plot, at the time of the peak torque the conventional engine has a much higher angularity. Another interesting observation also seen in the friction plot is that the Pettinger Engine has a higher negative friction particularly during the end of compression. This phenomenon can again be explained by the angularity plot. As evident, the angularity close to the end of compression for the conventional engine is much lower than that of the Pettinger Engine and thus there is

higher friction for Pettinger Engine. The less friction during the peak torque of the Pettinger Engine however is the important part from this analysis because it is the point when maximum power is being produced and less friction during that point certainly helps to reduce power loss.

*3.3.1 Effect of Angularity and Friction on Torque*

Our initial understanding was that less friction during the peak torque for the Pettinger Engine was causing the higher peak torque in the Pettinger Engine as was observed before. It seemed reasonable to make this assumption, but our later analysis showed that was not the case.

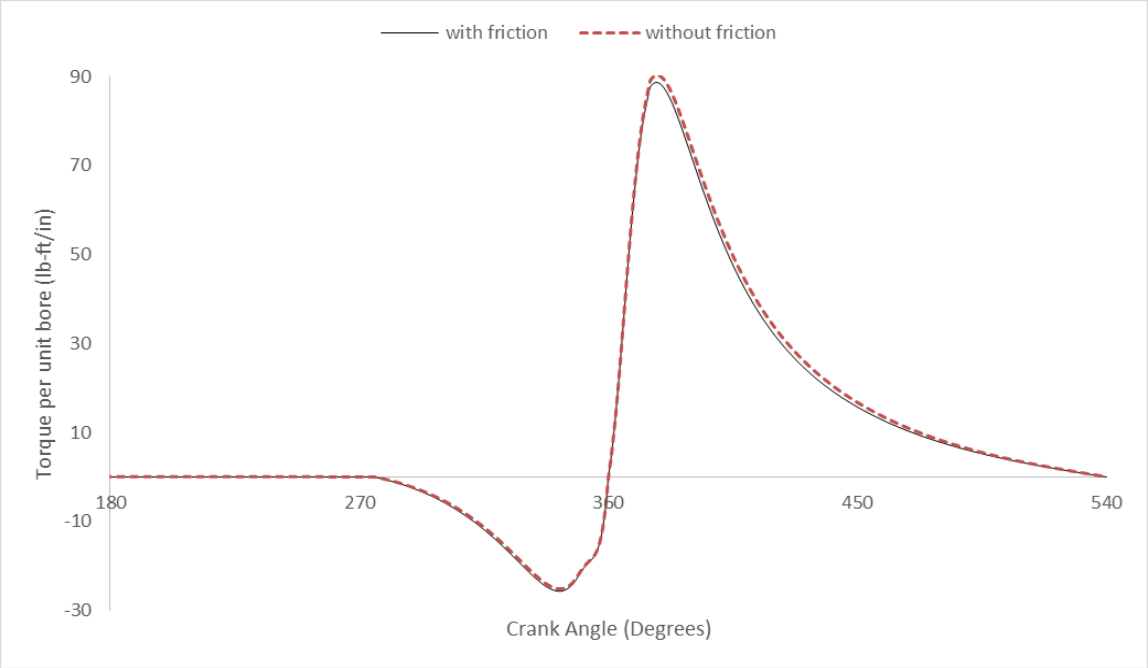


Figure 3.6: Torque with and without friction for conventional engine

Figure 3.6 is the torque for the conventional engine with and without friction. Our initial assumption was that the friction would play a major role in increasing the torque value. However, looking at the plot it seems obvious that it does not have much effect on

the torque at all. The plot for Pettinger Engine shown below in figure 3.7 shows that the friction had even less effect on the torque output. These results obviously seemed counter intuitive. One possible explanation to support this result is that the friction that we considered is only sliding friction. In a more realistic model, other friction such as the viscous friction, ring friction, internal friction, etc. also come in to play and thus the overall friction should have more impact on the torque (Pulkrabek). However, at the moment it looks as though more than the friction, the kinematics of the Pettinger Engine is itself causing higher torque. This means due to the complicated kinematics of the Pettinger Engine, the forces generated in the linkages are higher such that the reaction torque on the crank is itself higher giving a higher torque output. This is only an assumption and actual testing would be required to verify this claim.

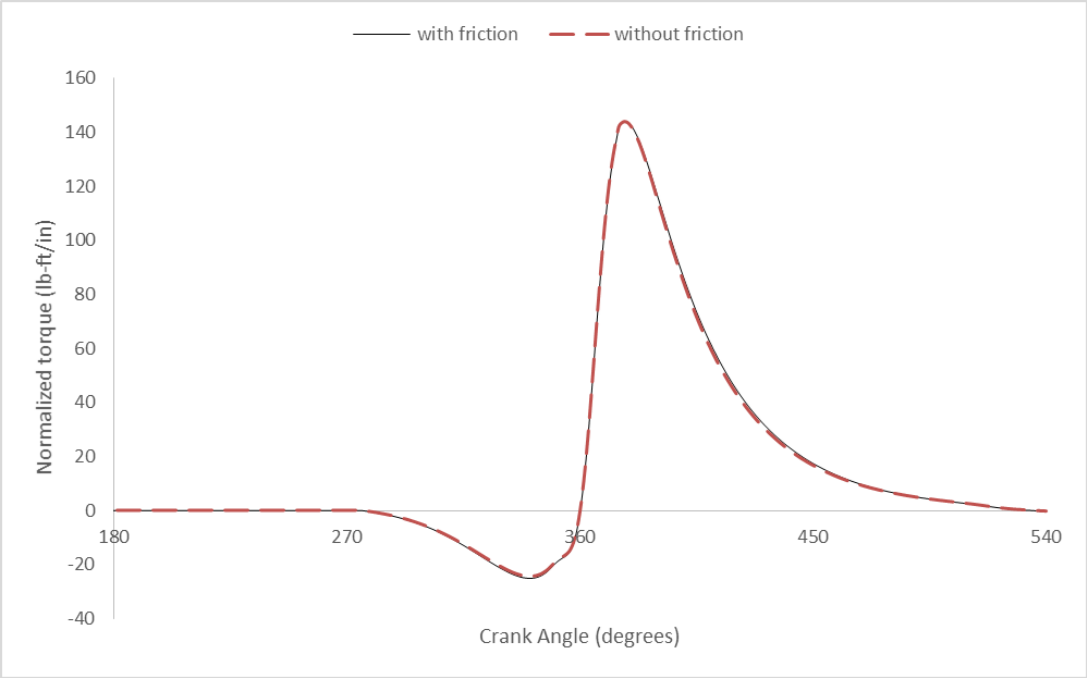


Figure 3.7: Torque with and without friction for the Pettinger Engine

CHAPTER 4

# THROTTLE ELIMINATION ANALYSIS

## 4.1 Pumping Loss

At lower throttles during the intake stroke, the piston has to pull against a partial vacuum. This causes valuable energy from the engine to be wasted. This waste of energy during the intake pumping cycle is called the pumping loss. Removal of this pumping loss can increase the output of an engine significantly ("Part Load Pumping Losses in an SI Engine."). It will be discussed later how the throttle blade can be completely removed to eliminate pumping. For now, we will discuss on how the pumping loss is actually calculated.

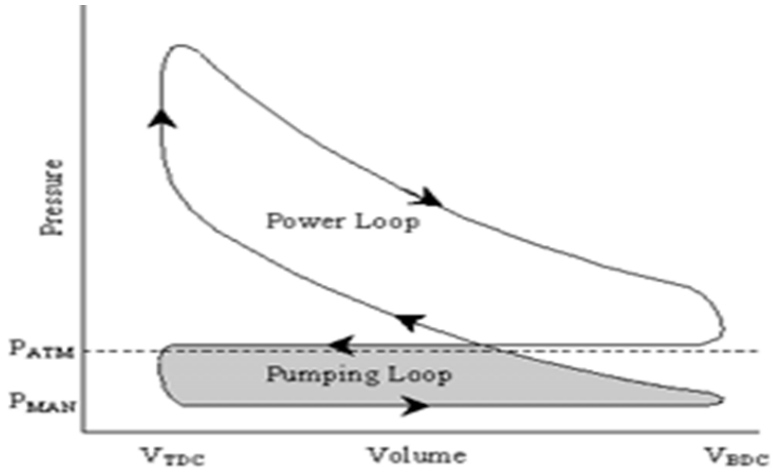


Figure 4.1: Pressure vs volume demonstrating the pumping loop and the power loop

Referring to figure 4.1, which is just a demonstration plot and not the actual plot, the pumping loop is enclosed by the intake, exhaust, and some compression cycle curves,

whereas the power loop is enclosed by the compression, expansion and some exhaust cycle curve. Simply saying, the pumping loss is just the area in the pumping loop that lies below the atmospheric pressure ("Part Load Pumping Losses in an SI Engine.").

Calculating the pumping loss is simply about determining how much percent is the pumping loop area as compared to the power loop area. Now, doing this is a little complicated than it seems. First Pressure is plotted against the cylinder volume, which gives a plot that starts at a particular volume and pressure and ends at the same point.

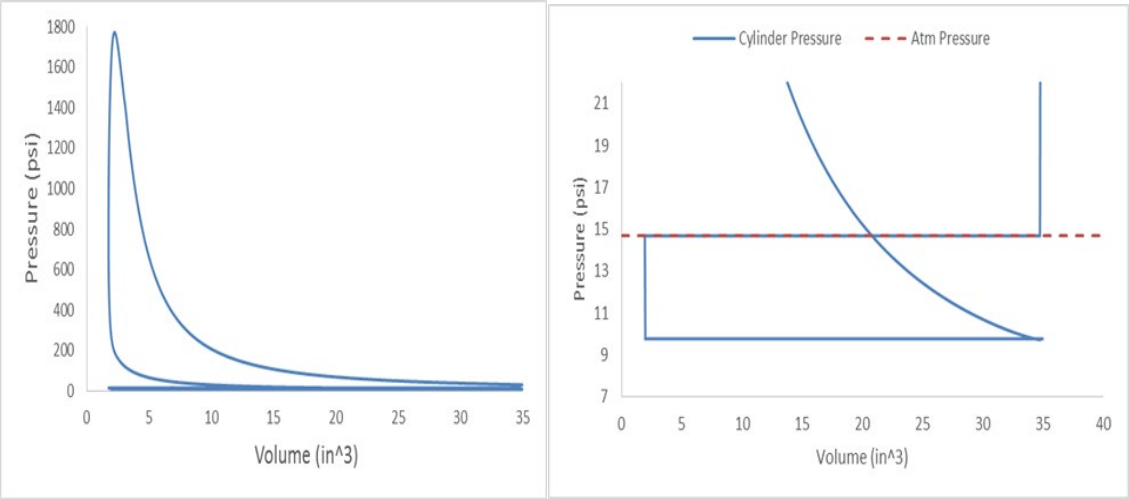


Figure 4.2: Cylinder pressure vs volume (left) and zoomed in at the pumping loop (right) for 50% throttle

Figure 4.2 is the actual plot obtained for 50% throttle. Similar plots were obtained for other throttles as well. After plotting pressure versus volume, curve fitting was done in excel to find equations of compression, combustion and expansion curves. The equations were then integrated over their respective volumes to obtain their respective area under the curves. Carefully subtracting the area obtained by the upper curve from the area obtained by the lower curve for the power loop and the pumping loop then gave the area inside the power loop and the pumping loop. The two areas in the PV graph are the

work produced for the power loop and work lost for the pumping loop. The pumping loss is then simply calculated by the following formula

$$pumping\ loss\ (\%) = \frac{A_{pumping\ loop}}{A_{Power\ loop}} \times 100$$

Figure 4.3 below shows the pumping loss as a function of throttle demand. The maximum pumping loss of about 7% occurs when the engine is idle, and then it starts to decrease. This decreasing trend is obvious because as the throttle demand increases, the intake pressure increases, which means less partial vacuum and thus, less pumping loss. The important thing to remember however is: whatever the percentage, power is being wasted and throttle elimination will completely eliminate such waste.

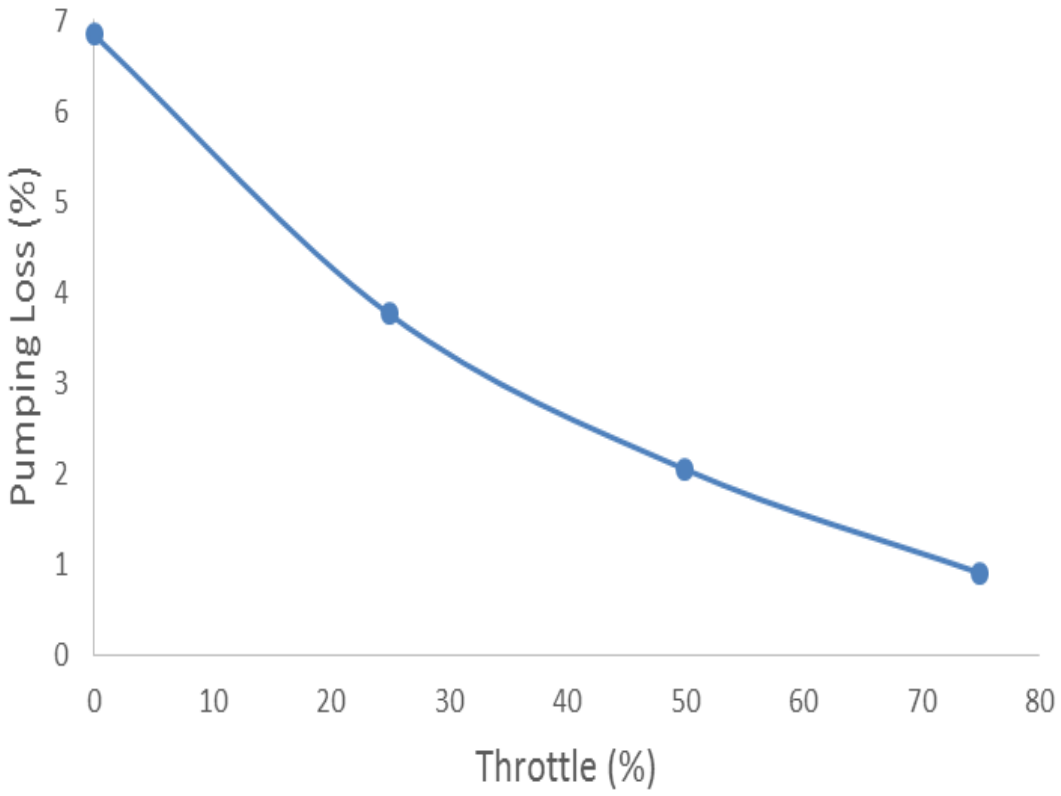


Figure 4.3: Pumping loss vs throttle demand

## 4.2 Intake Valve Timing

One way to eliminate pumping loss is by varying the crank angle at which the intake valve closes. In a traditional engine, the intake valve always closes at the same time. The amount of mass required for complete combustion for corresponding throttle demand is maintained by a throttle blade. However, as discussed earlier, the throttle blade introduces pumping losses, which are not desired. In the absence of throttle blade, the amount of mass required for complete combustion corresponding to the throttle demand can be obtained by varying the intake valve timing. The pressure in this case will always be atmospheric pressure. The amount of mass required for complete combustion using a throttle can be calculated and that same amount of mass can be used in the ideal gas equation to give the volume required for throttle less operation. The volume thus obtained can then be simply related to the crank angle when the intake valve should be closed.

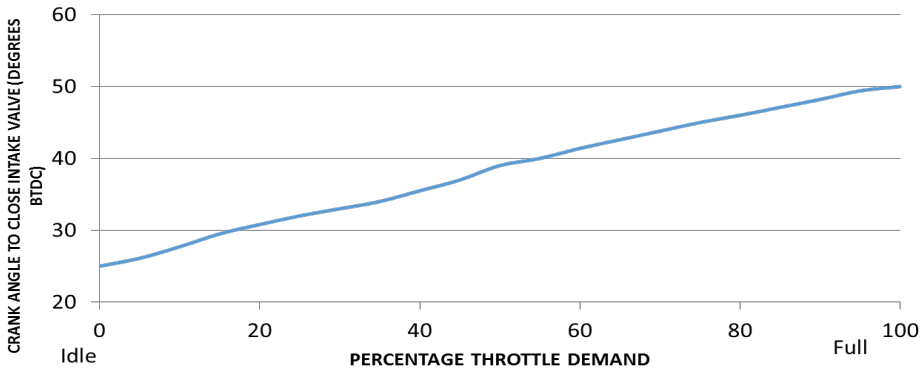


Figure 4.4: Intake valve timing vs throttle demand

Figure 4.4 shows the graph relating intake valve timing to the throttle demand. This plot was obtained by the method of analysis discussed earlier. By using this plot and the curve fit equation a control system to control the intake valve closing can thus be devised if desired.

# CHAPTER 5

# CONCLUSION

The Pettinger Engine has relatively higher peak torque when compared to a conventional engine of the same size. The angularity and friction comparisons of the Pettinger Engine and the conventional engine showed quite a lot of differences. However, the angularity and friction did not seem to have much effect on the torque of the Pettinger Engine as well as the conventional engine. It is thus assumed that the higher torque of the Pettinger Engine is due to its complicated kinematics and geometry. However, further experimentation must be done to prove this assumption. The implementation of Variable exhaust valve timing allowed for more work extraction due to variable expansion ratio. Finally, throttle elimination through intake valve timing allowed for the elimination of pumping losses.

# APPENDIX A

## LOTUS INTERFACE SCREENSHOT

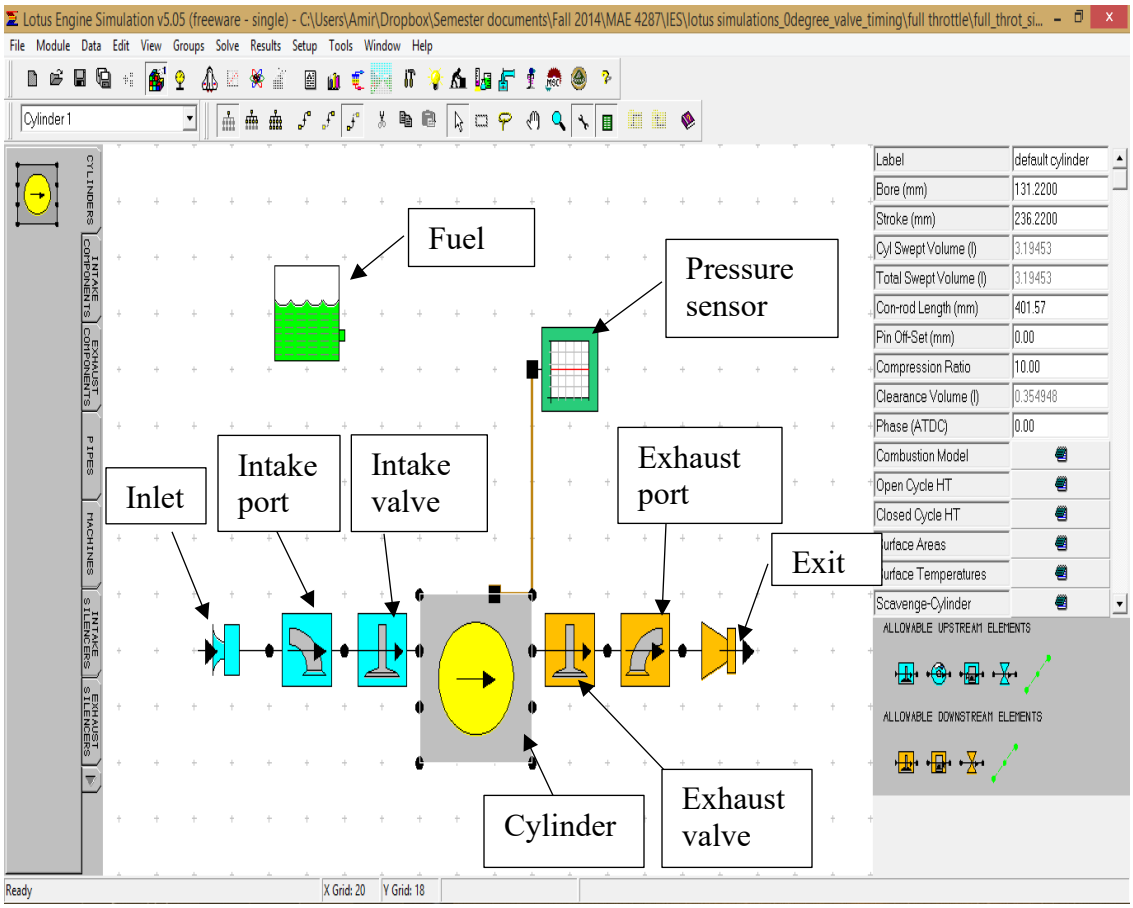


Figure A.1: Lotus software interface screenshot

# APPENDIX B

# PRESSURE THEORY SAMPLE CALCULATIONS

Known:

Throttle Position = full throttle

Bore, B= 5.166 in

Connecting rod length, r = 15.81 in

Stroke, S=9.3 in

Crank offset, a = 4.65 in

Dead volume, Vc = 11.467 in^3 (0.0001879 m^3)

Ignition angle = 12 degrees bTDC

End angle of combustion = 15 degrees aTDC (Pulkrabek)

The piston position from crank connection and total volume in the cylinder are given by the following respective equations (Pulkrabek)

$$s = acos\theta + \sqrt{r^2 - a^2 \sin^2 \theta} \qquad (1)$$

$$V = Vc + \left(\frac{\pi B^2}{4}\right)(r + a - s) \qquad (2)$$

Where θ = crank angle

Rearranging the volume equation gives

$$s = (r + a) - \frac{4 * (V - Vc)}{\pi B^2} \qquad (3)$$

For compression ratio of 10:1, the total volume, V = 114.67 in^3 (0.001879 m^3)

Substituting, the known values and the V above in the above equation gives s=15.53 in

Substituting s in equation (1) gives,

$$15.53 = 4.65cos\theta_2 + \sqrt{15.81^2 - 4.65^2 \sin^2 \theta_2}$$

Numerically solving this equation gives $\theta_2$=276 degrees which is the angle at which compression starts

At the start of compression,

P2=Patm=101325 N/m^2 (14.69 psi)  (for full throttle)

V2=114.67 in^3 = 0.001879 m^3

At the end of compression,

From polytropic equation

$$P_2V_2^n = P_3V_3^n \quad (4)$$

Since ignition angle is 12 degrees bTDC for full throttle, the crank angle at which combustion starts, θ3=348°

Substituting θ3 in equation 1 gives s3=20.32 in

Substituting s3 in equation 2 then gives v3=14.401 in^3 (0.0002359 m^3)

Now, from equation 4, $P_3 = P_2\left(\frac{V_2}{V_3}\right)^n$

$$P_3 = 14.69\left(\frac{114.67}{14.401}\right)^{1.3}$$

$$P_3 = 217.969\ psi\ (1502843.288\frac{N}{m^2})$$

Using cold air standard assumptions for the air fuel mixture,

Temperature at the start of compression (T2) = 298 K (room temperature)

From ideal gas law,

$$P_2V_2 = nRT_2$$

$$P_2V_2 = \frac{m_{total}}{Mair}RT$$

Where Mair = molar mass of air = 28.97*10^-3 kg/mol

$$m_{total} = \frac{P_2V_2M_{air}}{RT_2}$$

$$m_{total} = \frac{101325 \times 0.001879 \times 28.97 \times 10^{-3}}{8.314 \times 298}$$

$$m_{total} = 0.00222\ kg = 2.22\ g$$

The Air fuel ratio (AF) = 14.7

$$m_{air} + m_{fuel} = m_{total}$$

Substituting AF=mair/mfuel and rearranging gives

$$m_{fuel} = \frac{m_{total}}{AF + 1}$$

$$m_{fuel} = 0.1414\ g = 0.1414 \times 10^{-3}\ kg$$

Cv of air at room temperature = 1.004 KJ/Kg.K (Cengel)

Now to find final temperature of combustion (Tf),

$$m_{total}Cv\left(T_f - T_{spark}\right) = Cm_{fuel}Q_{Hv}$$

Rearranging this equation gives

$$T_f = T_{spark} + \frac{Cm_{fuel}QHv}{m_{total}Cv} \qquad (5)$$

Here C=0.95

Again from ideal gas law at the start of combustion we have,

$$T_3 = \frac{P_3V_3M_{air}}{m_{total}R}$$

$$T_3 = \frac{1502843.288 \times 0.0002359 \times 28.97 \times 10^{-3}}{0.00222 \times 8.314} = 556.45\ K$$

Substituting T3 = Tspark in equation (5) gives, Tf=3208.23 K = T4

The end of combustion was defined as 15 degrees after TDC so θ4 = 375° which when substituted in equation 1 gives s4 = 20.25 in. Substituting s4 in equation 2 then gives V4 = 15.86 in^3 (0.0002598 m^3)

Now using ideal gas relation once again the pressure at the end of combustion, Pf can be found

$$P_2 = \frac{m_{total}}{V_4Mair}RT_4$$

Substituting V4 and T4 then gives, P4 = 1141.09 psi = Pf

Now that all the parameters required for combustion have been found, the pressure at any instant during combustion can be found by the combination of the following Weibe function and MLK model

$$Xb = 1 - \exp\left[-a\left(\frac{\theta - \theta o}{\Delta\theta}\right)^{m-1}\right.$$

$$P = \frac{X_b\left(P_fV_f^n - P_0V_0^n\right) + P_oV_0^n}{V^n}$$

Here θ0 = θ3 and $\Delta\theta$ = θ4-θ3

# APPENDIX C

# KINEMATIC ANALYSIS

Velocity Analysis

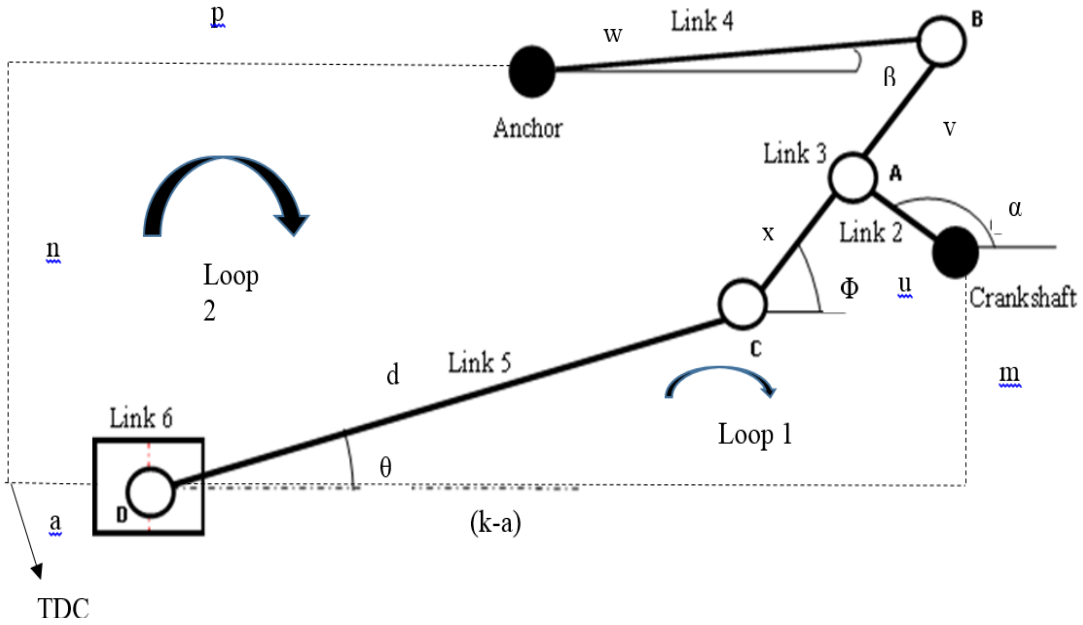


Figure C.1: Linkage configuration of the Pettinger Engine showing vector loops

Loop 1

$$de^{j\theta} + xe^{j\phi} - ue^{j\alpha} - jm - (k - a) = 0$$

Taking derivative of the equation,

$$dj\omega_5 e^{j\theta} + xj\omega_3 e^{j\phi} - uj\omega_2 e^{j\alpha} + \dot{a} = 0$$

$$dj\omega_5(cos\theta + jsin\theta) + xj\omega_3(cos\phi + jsin\phi) - uj\omega_2(cos\alpha + jsin\alpha) + \dot{a} = 0$$

Separating into real and imaginary part,

$$\boxed{\begin{aligned} &Imaginary: d\omega_5 cos\theta + x\omega_3 cos\phi - u\omega_2 cos\alpha = 0 \\ &Real: \ -d\omega_5 sin\theta - x\omega_3 sin\phi + u\omega_2 sin\alpha + \dot{a} = 0 \end{aligned}}$$

Loop 2

$$a + de^{j\theta} + le^{j\phi} - we^{j\beta} - p - jn = 0$$

Taking derivative of the equation,

$$\dot{a} + dj\omega_5 e^{j\theta} + lj\omega_3 e^{j\phi} - wj\omega_4 e^{j\beta} = 0$$

$$\dot{a} + dj\omega_5(cos\theta + jsin\theta) + lj\omega_3(cos\phi + jsin\phi) - wj\omega_4(cos\beta + jsin\beta) = 0$$

Separating into real and imaginary part,

$$Imaginary: d\omega_5 cos\theta + l\omega_3 cos\phi - w\omega_4 cos\beta = 0$$

$$\dot{a} - d\omega_5 sin\theta - l\omega_3 sin\phi + w\omega_4 sin\beta = 0$$

Putting the obtained velocity equations in matrix form,

$$\begin{bmatrix} dcos\theta & xcos\phi & 0 & 0 \\ -dsin\theta & -xsin\phi & 0 & 1 \\ dcos\theta & lcos\phi & -wcos\beta & 0 \\ -dsin\theta & -lsin\phi & wsin\beta & 1 \end{bmatrix} \times \begin{bmatrix} \omega_5 \\ \omega_3 \\ \omega_4 \\ \dot{a} \end{bmatrix} = \begin{bmatrix} u\omega_2 cos\alpha \\ -u\omega_2 sin\alpha \\ 0 \\ 0 \end{bmatrix}$$

Solving the above matrix, all the unknown velocity parameters can be calculated. Of particular interest is the velocity of piston ($\dot{a}$) because the sign of it determines whether the coefficient of friction is positive or negative.

Force Analysis

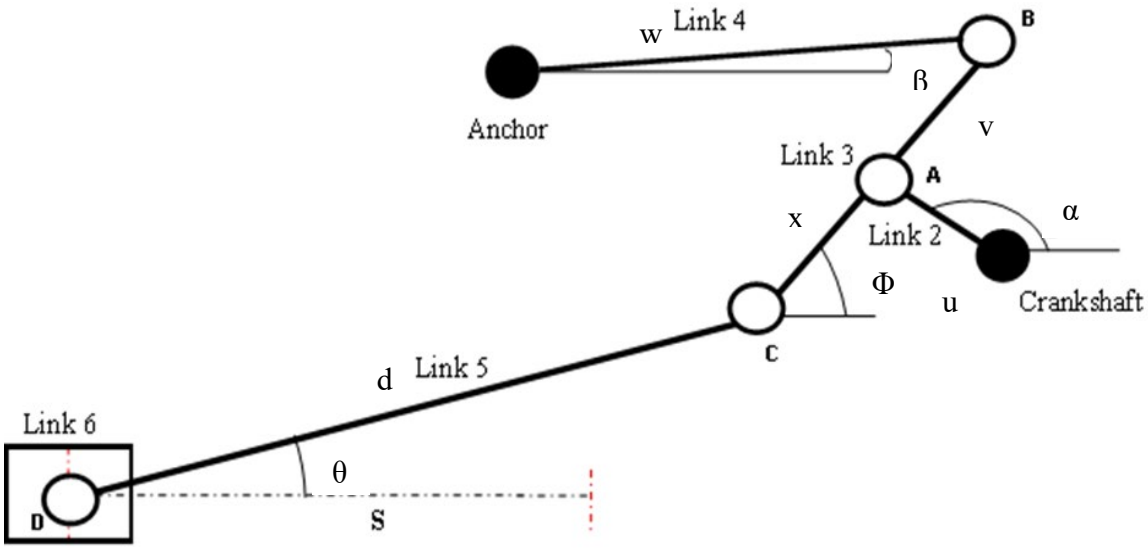


Figure**:** Linkage configuration of the Pettinger Engine

The force analysis performed below is a static force analysis because the force due to masses of the links were assumed to be insignificant when compared to the forces in the joints.

Link 2

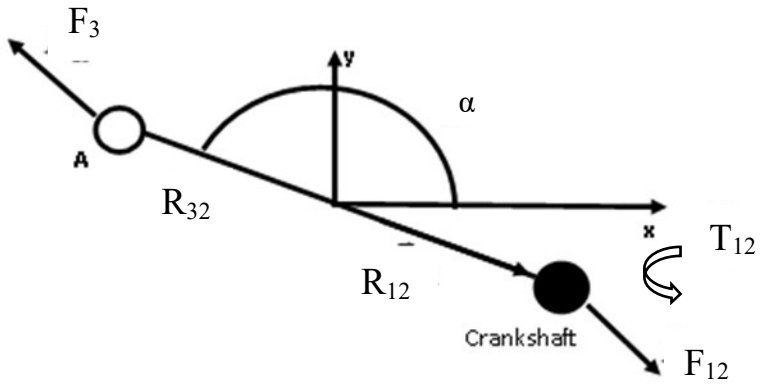


Figure: Free body diagram of link 2

$$\Sigma F_x = 0$$

$$F_{32x} + F_{12x} = 0 \quad (1)$$

$$\Sigma F_y = 0$$

$$F_{32y} + F_{12y} = 0 \quad (2)$$

$$\Sigma M = 0$$

$$T_{12} + [R_{12x}F_{12y} - R_{12y}F_{12x}] + [R_{32x}F_{32y} - R_{32y}F_{32x}] = 0 \quad (3)$$

Link 3

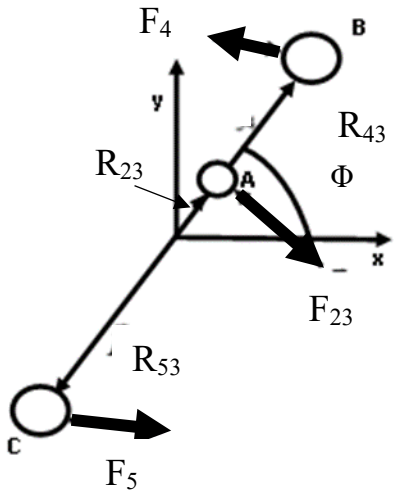


Figure: FBD of link 3

$$\Sigma F_x = 0$$

$$F_{53x} + F_{23x} + F_{43x} = 0$$

$$But, \qquad F_{23x} = -F_{32x}$$

$$So, \qquad \boxed{F_{53x} - F_{32x} + F_{43x} = 0 \quad (4)}$$

$$\Sigma F_y = 0$$

$$F_{53y} + F_{23y} + F_{43y} = 0$$

$$But, \qquad F_{23y} = -F_{32y}$$

$$So, \qquad \boxed{F_{53y} - F_{32y} + F_{43y} = 0 \quad (5)}$$

$$\Sigma M = 0$$

$$(R_{53x}F_{53y} - R_{53y}F_{53x}) + (R_{23x}F_{23y} - R_{23y}F_{23x}) + (R_{43x}F_{43y} - R_{43y}F_{43x}) = 0$$

,

$$But, \qquad F_{23x} = -F_{32x}$$

$$And, \qquad F_{23y} = -F_{32y}$$

$$So, \qquad \boxed{\begin{array}{l}(R_{53x}F_{53y} - R_{53y}F_{53x}) - (R_{23x}F_{32y} - R_{23y}F_{32x}) + (R_{43x}F_{43y} - R_{43y}F_{43x}) \\ \\ \qquad = 0 \quad (6)\end{array}}$$

Link 4

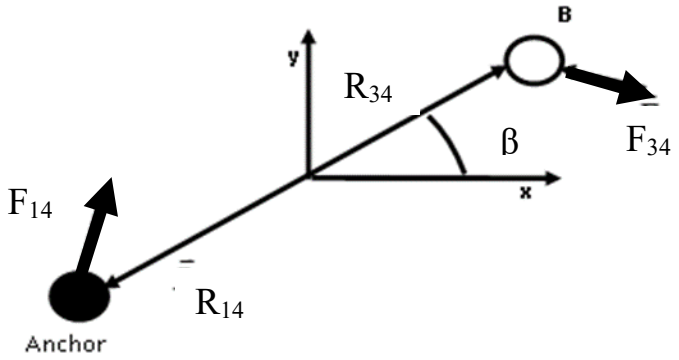


Figure: FBD of link 4

$$\Sigma F_x = 0$$

$$F_{14x} + F_{34x} = 0$$

$$\Sigma F_y = 0$$

$$F_{14y} + F_{34y} = 0$$

$$But, \qquad F_{34} = -F_{43}$$

$$So, \quad \boxed{F_{14x} - F_{43x} = 0 \quad (7)}$$

$$And, \quad \boxed{F_{14y} - F_{43y} = 0 \quad (8)}$$

$$\Sigma M = 0$$

$$\left(R_{14x}F_{14y} - R_{14y}F_{14x}\right) + \left(R_{34x}F_{34y} - R_{34y}F_{34x}\right) = 0$$

$$But, \qquad F_{34} = -F_{43}$$

$$So, \quad \boxed{\left(R_{14x}F_{14y} - R_{14y}F_{14x}\right) - \left(R_{34x}F_{43y} - R_{34y}F_{43x}\right) = 0 \quad (9)}$$

Link 5

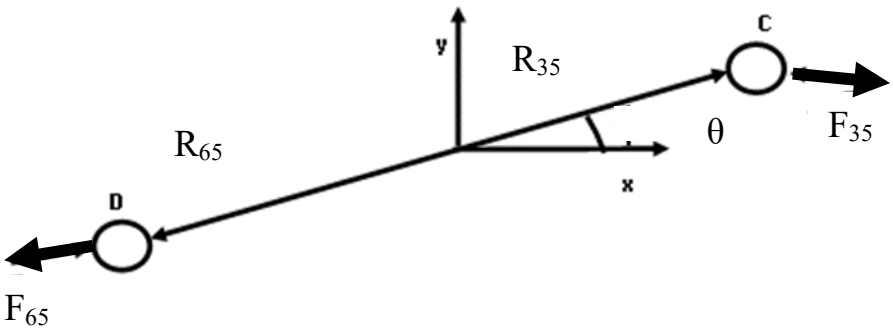


Figure: FBD of link 5

$$\Sigma F_x = 0$$

$$F_{65x} + F_{35x} = 0$$

$$\Sigma F_y = 0$$

$$F_{65y} + F_{35y} = 0$$

$$But, \quad F_{35} = -F_{53}$$

$$So, \quad \boxed{F_{65x} - F_{53x} = 0 \quad (10)}$$

$$And, \quad \boxed{F_{65y} - F_{53y} = 0 \quad (11)}$$

$$\Sigma M = 0$$

$$\left(R_{65x}F_{65y} - R_{65y}F_{65x}\right) + \left(R_{35x}F_{35y} - R_{35y}F_{35x}\right) = 0$$

$$But, \quad F_{35} = -F_{53}$$

$$So, \quad \boxed{\left(R_{65x}F_{65y} - R_{65y}F_{65x}\right) - \left(R_{35x}F_{53y} - R_{35y}F_{53x}\right) = 0 \quad (12)}$$

Link 6

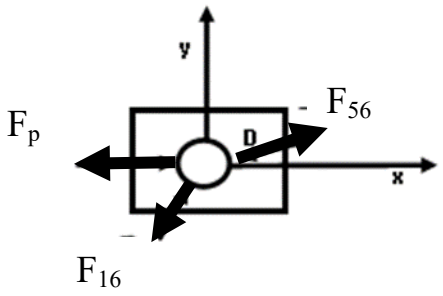


Figure: FBD of link 6 (Piston)

$$\Sigma F_x = 0$$

$$F_{px} + F_{16x} + F_{56x} = 0$$

$$\Sigma F_y = 0$$

$$F_{py} + F_{16y} + F_{56y} = 0$$

$$But, \quad F_{56} = -F_{65}$$

$$So, \quad F_{px} + F_{16x} - F_{65x} = 0$$

$$And, \quad F_{py} + F_{16y} - F_{65y} = 0$$

$$Also, \quad F_{16x} = \mu F_{16y} \; and \; F_{py} = 0$$

Note that the sign of μ is always opposite to the sign of velocity of the piston.

$$So, \quad \boxed{\begin{aligned} &F_{px} + \mu F_{16y} - F_{65x} = 0 \quad (13) \\ &F_{16y} - F_{65y} = 0 \quad (14) \end{aligned}}$$

Radius determination

$$R_{12} = R_{32} = \frac{u}{2}$$

$$R_{12x} = R_{12}Cos(\alpha + 180°)$$

$$R_{12y} = R_{12}Sin(\alpha + 180°)$$

$$R_{32x} = R_{32}Cos(\alpha)$$

$$R_{32y} = R_{32}Sin(\alpha)$$

$$R_{53} = \frac{l}{2} \qquad R_{23} = \left(\frac{l}{2} - v\right) \qquad R_{43} = l - R_{53} \qquad l = x + v$$

$$R_{53x} = R_{53}Cos(\phi + 180°)$$

$$R_{53y} = R_{53}Sin(\phi + 180°)$$

$$R_{23x} = R_{23}Cos(\phi)$$

$$R_{23y} = R_{23}Sin(\phi)$$

$$R_{43x} = R_{43}Cos(\phi)$$

$$R_{43y} = R_{43}Sin(\phi)$$

$$R_{34} = R_{14} = \frac{w}{2}$$

$$R_{34x} = R_{34}Cos(\beta)$$

$$R_{34y} = R_{34}Sin(\beta)$$

$$R_{14x} = R_{14}Cos(\beta + 180°)$$

$$R_{14y} = R_{14}Sin(\beta + 180°)$$

$$R_{35} = R_{65} = \frac{d}{2}$$

$$R_{35x} = R_{35}Cos(\theta)$$

$$R_{35y} = R_{35}Sin(\theta)$$

$$R_{65x} = R_{65}Cos(\theta + 180°)$$

$$R_{65y} = R_{65}Sin(\theta + 180°)$$

The above 14 equations from the force equations can be put in a matric form as follows

Force Matrix

$$\begin{bmatrix}
1 & 0 & 0 & 0 & 0 & 1 & 0 & 0 & 0 & 0 & 0 & 0 & 0 & 0 \\
0 & 1 & 0 & 0 & 0 & 0 & 1 & 0 & 0 & 0 & 0 & 0 & 0 & 0 \\
-R_{12y} & R_{12x} & 0 & 0 & 0 & -R_{32y} & R_{32x} & 0 & 0 & 0 & 0 & 0 & 0 & 1 \\
0 & 0 & 0 & 0 & 0 & -1 & 0 & 1 & 0 & 1 & 0 & 0 & 0 & 0 \\
0 & 0 & 0 & 0 & 0 & 0 & -1 & 0 & 1 & 0 & 1 & 0 & 0 & 0 \\
0 & 0 & 0 & 0 & 0 & R_{23y} & -R_{23x} & -R_{43y} & R_{43x} & -R_{53y} & R_{53x} & 0 & 0 & 0 \\
0 & 0 & 1 & 0 & 0 & 0 & 0 & -1 & 0 & 0 & 0 & 0 & 0 & 0 \\
0 & 0 & 0 & 1 & 0 & 0 & 0 & 0 & -1 & 0 & 0 & 0 & 0 & 0 \\
0 & 0 & -R_{14y} & R_{14x} & 0 & 0 & 0 & R_{34y} & -R_{34x} & 0 & 0 & 0 & 0 & 0 \\
0 & 0 & 0 & 0 & 0 & 0 & 0 & 0 & 0 & -1 & 0 & 1 & 0 & 0 \\
0 & 0 & 0 & 0 & 0 & 0 & 0 & 0 & 0 & 0 & -1 & 0 & 1 & 0 \\
0 & 0 & 0 & 0 & 0 & 0 & 0 & 0 & 0 & R_{35y} & -R_{35x} & -R_{65y} & R_{65x} & 0 \\
0 & 0 & 0 & 0 & \mu & 0 & 0 & 0 & 0 & 0 & 0 & -1 & 0 & 0 \\
0 & 0 & 0 & 0 & 1 & 0 & 0 & 0 & 0 & 0 & 0 & 0 & -1 & 0
\end{bmatrix}$$

$$\times$$

$$\begin{bmatrix}
F_{12x} \\ F_{12y} \\ F_{14x} \\ F_{14y} \\ F_{16y} \\ F_{32x} \\ F_{32y} \\ F_{43x} \\ F_{43y} \\ F_{53x} \\ F_{53y} \\ F_{65x} \\ F_{65y} \\ T_{12}
\end{bmatrix} = \begin{bmatrix}
0 \\ 0 \\ 0 \\ 0 \\ 0 \\ 0 \\ 0 \\ 0 \\ 0 \\ 0 \\ 0 \\ -F_{px} \\ 0
\end{bmatrix}$$

Solving the above matrix, the required parameters can be obtained. The torque output required for instance is $T_{12}$.

# APPENDIX D

# PUMPING LOSS SAMPLE CALCULATION

Pumping Loss Sample Calculation of 25% throttle

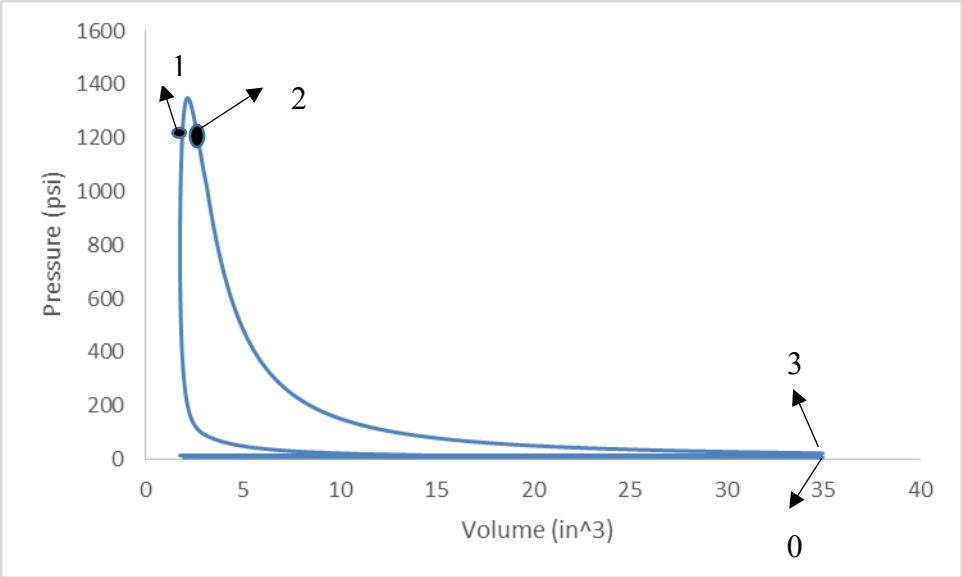


Figure D.1: Pressure vs volume for 25% throttle

In figure above the loop 0-1-2-3 is the power loop, the area enclosed in this power loop can be found by subtracting the area of 0-1 from 1-2 and 2-3. The equation of the curves in these sections were found by curve fitting. These equations were then integrated within the respective volume to get the areas.

Equation of curve 0-1after curve fitting is found to be $P = 691.14\, V^{-1.356}$

Where P is the pressure and V is the volume

Similarly, equation of curve 1-2 is $P = -1083\, V^2 + 4697\, V - 3742.9$

And, the equation of curve 2-3 is $P = 5767.1\, V^{-1.564}$

The area under the curves are then found as follows.

$$A_{0-1} = \int_{1.97}^{34.7} 691.14\, V^{-1.356}\, dV = 975.821$$

$$A_{1-2} = \int_{1.97}^{2.34} -1083\, V^2 + 4697\, V - 3742.9\ dV = 494.801$$

$$A_{2-3} = \int_{2.34}^{34.7} 5767.1\, V^{-1.564}\, dV = 4947.19$$

The area of the power loop,

$$A_{po} = A_{1-2} + A_{2-3} - A_{0-1} = 4466.17$$

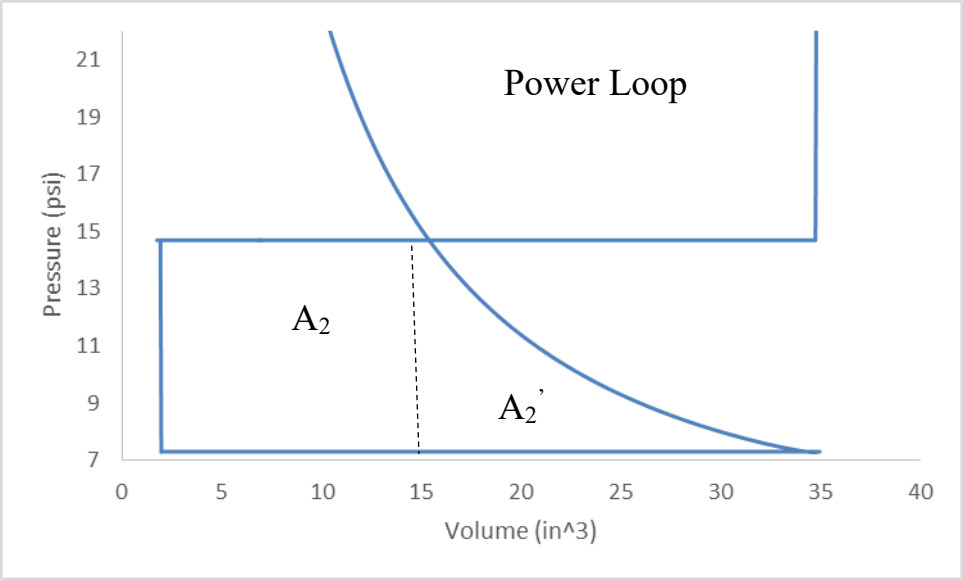


Figure D.2: Zoomed in pressure vs volume for 25% throttle showing the pumping loop

In the figure above, the area of pumping loop can be found by adding areas $A_2$ and $A_2'$. $A_2$ is a rectangle, whereas $A_2'$ can be approximated as a triangle. They are calculated as follows:

$$A_2' = \frac{1}{2} \times (34.7 - 14.8) \times (14.69 - 7.304) = 73.49$$

$$A_2 = (14.69 - 7.304) \times (14.8 - 1.97) = 94.76$$

Thus, area of pumping loop is

$$A_{pu} = A_2' + A_2 = 168.25$$

Therefore, pumping loss can simply be calculated as

$$Pumping\ loss\ (\%) = \frac{A_{pu}}{A_{po}} \times 100\% = \frac{168.25}{4466} \times 100\% = \boxed{3.76\%}$$

# APPENDIX E

# DIMENSIONAL REDUCTION THEORY

To get a comparable value of the results, the bore size and stroke to bore ratio were reduced to a reasonable values as discussed earlier in the report. It was found that when the bore was reduced from B=5.166 inch to B=3.27 inch and stroke to bore ratio reduced from S/B=1.8 to S/B=1.2, the crank offset, reduced from a=4.65 inch to a=1.96 inch.

The reduction factor was thus calculated as $rf = \frac{1.96}{4.65} = 0.421$

The reduction factor when multiplied to the previous dimension of the Pettinger Engine gave the required new dimensions. By using this method the dimensions can be adjusted easily instead of doing another linkage synthesis.

A simple proof is shown below to prove that this dimension reduction method works every time.

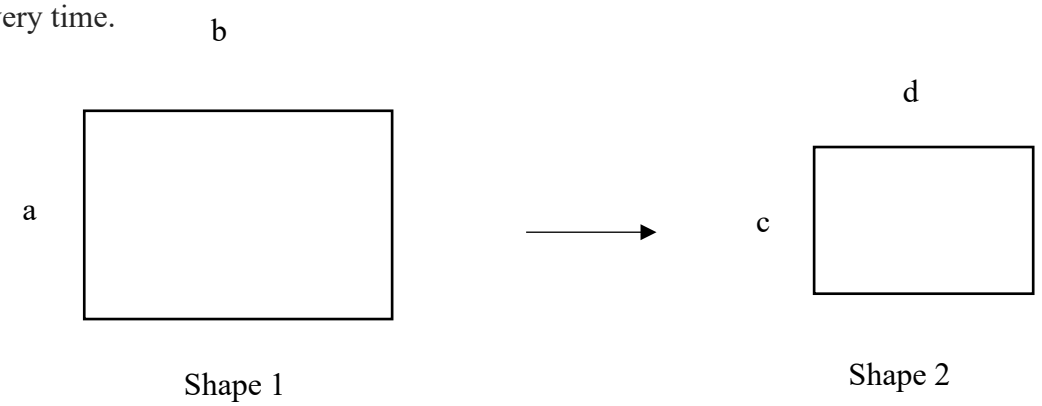


Consider that the dimensions of shape 1 is proportionally reduced to shape 2.

Let the reduction factor be

$$rf = \frac{c}{a}$$

The according to the assumed theory,

$$d = b \times \frac{c}{a}$$

The ratio of d/b is then

$$\frac{d}{b} = \frac{b \times \frac{c}{a}}{b} = \frac{c}{a}$$

This simple analysis proves that if the dimensions of the shapes are reduced proportionally then the factor by which each of the dimensions are reduced is always the same.z

REFERENCES

Cengel, B. *Thermodynamics: An Engineering Approach*. Seventh Edition. 7th. McGraw-Hill Company, 2010.

HRTuning. Neptune RTP. Computer software. HRTuning - Home Of The NepTune RTP. Vers. 10. HRTuning, 1 Jan. 2001. Web. 06 Nov. 2014. <http://www.hrtuning.com/pages/category/neptune-rtp>.

Innovative Engine Solutions (IES). *Pettinger Engine: Analysis and Variable Valve Timing*. Rep. N.p.: n.p., 2014. Print.

Kuo, Paulina S. "Cylinder Pressure in a Spark-Ignition Engine: A Computational Model." J. Undergrad (n.d.): n. pag. 1996. Web. 22 Nov. 2014. <http://www.hcs.harvard.edu/~jus/0303/kuo.pdf>.

Lotus Cars Ltd. "Getting Started Using Lotus Engine Simulation." (2001): 25-26. Web. 28 Nov. 2014. http://lotusproactive.files.wordpress.com/2013/08/getting-started-with-lotus-engine-simulation.pdf

Norton, R. L. *Design of Machinery: An Introduction to the Synthesis and Analysis of Mechanisms and Machines*. 5th Edition. McGraw-Hill, n.d.

Pace, Brandi, Jared Wiggins, and John Sandberg. A Brief Look into the Variations of Internal Combustion Engines and the Physics That Make Them Run. Thesis. Salt Lake Community College, 2011. N.p.: n.p., n.d. Print.

"Part Load Pumping Losses in an SI Engine." Mechadyne International. N.p., 2012. Web. 04 May 2015. <http://www.mechadyne-int.com/vva-reference/part-load-pumping-losses-si-engine>.

Pettinger, Wesley. *The Pettinger Cycle; Energy Conversion For the Benefit of Humanity; A Different Internal Combustion Engine*. N.p.: n.p., 2013. PPT.

Pulkrabek, Willard W. *Engineering Fundamentals of the Internal Combustion Engine.* Upper Saddle River, NJ: Pearson Prentice Hall, 2004. Print.

System Power Analysis and Research of Combustion (SPARC). *Pettinger Engine: Analysis and Improvement*. Rep. N.p.: n.p., 2014. Print.

## BIOGRAPHICAL INFORMATION

Amir Shrestha is an undergraduate student at the University of Texas at Arlington. He is a Mechanical Engineering senior and is expected to graduate in Spring 2015 with an Honors Bachelor of Science in Mechanical Engineering. His research interests are in the field of engine performance, automobile, machine design and kinematics and dynamics. He has worked on numerous projects, notably the analysis of the Pettinger Engine, stress and thermal analysis of an automobile brake caliper, control system design of an active control pantograph, and gear system design for a hoist. He plans to do graduate study in Mechanical Engineering and eventually become an engineering professional.